# Experimental analysis of short concrete column under hygrothermo-mechanical accelerated aging

Nacera Hassani, Hocine Dehmous
*University Mouloud Mammeri of Tizi-Ouzou, Algeria*
*nacera.hassani@ummto.dz,*
*hocine.dehmous@ummto.dz, https://orcid.org/0000-0001-7522-7363*

**ABSTRACT.** Concrete is still considered to be very durable material for a long time. However many constructions have shown degradations during their service life. To ensure safety, stability and serviceability of civil engineering structures, understanding of deterioration processes and their effect on the residual structural load capacity is necessary. This paper is based on the experimental study of short prismatic concrete columns under the hygrothermo-mechanical aging process. To investigate the effects of the exposure conditions on the strength of specimens, combined Ultrasonic Pulse Velocity testing and compression loading testing was used. It can be observed from the results obtained in this work that the ultrasonic pulse velocity measurements agree well with the experimental results obtained from the compression loading testing. Results indicate that in first time, degradation of specimens occurs slightly. After that the degradation becomes notable. It also indicates that the degradation due to the combined effect of the hygrothermo-mechanical aging process is higher than when we consider hygrothermal and mechanical process separately.

**KEYWORDS.** Short Concrete column; Hygrothermo-mechanical aging; Ultrasonic pulse velocity; Compression testing.

# INTRODUCTION

Due to its high strength, cost, and durability, reinforced cement concrete has been for many years, the first choice to be used as a building material. In fact, concrete structures are characterized by their relatively long durability. However, as a result of mechanical and chemical attacks (load-unload, temperature/moisture fluctuations, corrosion of reinforcement), premature failure of structure is often observed. Sanjeev Kumar Verma et al. proposed a simple diagram, shown in Fig.1, to illustrate the process of deterioration, reduction in strength and service life of an existing structure during its in-service [1]. It can be seen from this figure that residual life of a concrete structure at current

time depends on the present performance, rate of deterioration and minimum acceptable performance [1]. To ensure safety, stability and serviceability of civil engineering structures, continuous structural monitoring of these structures is necessary [2].To perform quantitative predictions of the service life of civil engineering structures, it is essential to better understand the mechanisms of the different degradations processes and their kinetics [3]. Generally, damaging of a concrete structure comprises two successive stages [4, 5, 6]; the first named a latent stage corresponds to the slow concrete damage, without any visible effects. The second named a propagation stage of the material damages and in which damages are visible. Several research papers have focused on the influence of environmental factors on concrete structure elements [7, 8, 9]. This was done either by considering the separated effect of mechanical loading and the hygrothermal exposure [10, 11, 12, 13, 14] or by considering the combined effect of the hygrothermo-mechanical conditions [15, 16, 17, 18, 20]. In addition, researchers consider normalized specimens which don't represent a reality in term of slenderness ratio h/b where h and b represent respectively the height and the width of specimens, as is show in the recent review published by OlaAdel Qasim [20]. Furthermore, to consider the mechanical loading, researchers often consider the ultimate load capacity (yielding point of concrete element) [16].
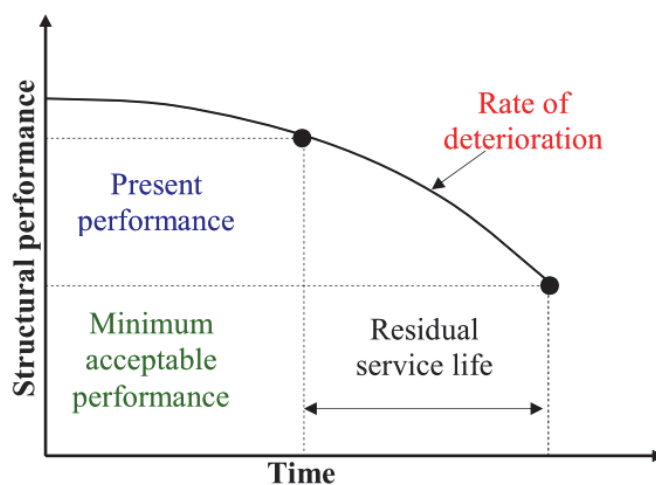


Figure 1: Deterioration process of structural performance over a period of time [1].

In this work, we report on the experimental analysis of short concrete columns under the combined effects of the thermal (temperature), hygric (moisture) and mechanical (displacement) aging. In addition, for more realistic evaluation, we propose a mechanical aging process (load-unload) by considering the design strength according to the technical standards related to the design of concrete structure instead of the ultimate strength [21]. We also report on the effect of slenderness ratio h/b. Finally, to quantify degradation of specimens, we combine ultrasonic pulse velocity test (UPV) as non-destructive testing (NDT)and compression loading test as destructive testing (DT).

## MATERIALS AND EXPERIMENTAL PROGRAM

### Materials

Twenty seven short prismatic columns specimens were prepared from the same concrete mixture, using Portland cement CPJ-CEM II/B 42.5 N, natural river sand (fine aggregates) and crushed gravels (coarse aggregates). Tap water was used for mixing and curing. The mix proportion used is shown in Tab. 1. To characterize the concrete used in this study, three prismatic specimens were prepared from the mixed concrete and tested at an age of 90 days. The density and the ultimate strength labeled Ru of the concrete measured in the axial compression test are summarized in Tab. 2.

.

| Sand 0-3 [mm] | Gravel 3-8 [mm] | Gravel 8-15 [mm] | Cement | Water | W/C ratio |
|---|---|---|---|---|---|
| 621 | 370 | 850 | 350 | 182 | 0.52 |

Table 1: Concrete mixture proportions [kg/m³].

| Properties | Specimens | | | Mean | Standard deviation |
|---|---|---|---|---|---|
| | 1 | 2 | 3 | | |
| Density [kg/m³]×10³ | 2.35 | 2.39 | 2.35 | 2.36 | 0.018 |
| Ultimate strength [KN] | 118.6 | 127.85 | 111.62 | 119.35 | 6.647 |

Table 2: Density and compressive strength results (after 90 days).

## Specimens preparation and grouping

Twenty one prismatic specimens with dimensions of 7cm×7cm×28cm, were prepared and organized into three groups according to the exposures conditions. In addition, in order to analyze the effect of the slenderness ratio, three prismatic specimens with dimensions of 7cm×7cm×14cm and three prismatic specimens with dimensions of 7cm×7cm×7cm were prepared. Details of specimens used in this study are shown in the Tab. 3.

| Group | Notation | Hygro-thermal exposure | Mechanical exposure Load-Unload | h/b ratio | Number of specimens |
|---|---|---|---|---|---|
| Group I | SC-I | Yes | No | 4 | 3 |
| Group II | SC-II-30 | No | 30% of Rd | 4 | 3 |
| | SC-II-50 | No | 50% of Rd | 4 | 3 |
| | SC-II-70 | No | 70% of Rd | 4 | 3 |
| Group III | SC-III-30 | Yes | 30% of Rd | 4 | 3 |
| | SC-III-50 | Yes | 50% of Rd | 4 | 3 |
| | SC-III-70 | Yes | 70% of Rd | 4 | 3 |
| Group IV | SC-IV70 | Yes | 70% of Rd | 2 | 3 |
| Group V | SC-V70 | Yes | 70% of Rd | 1 | 3 |

Table 3: Detailed grouping of short column specimens.

## Hygrothermo-mechanical aging process

Hygrothermal conditions consist of: first, immersion in tap water for 24 hours, second, evaporation of excess water in ambient air temperature for 24 hours and finally temperature cure cycle as shown in Fig. 2. Detailed temperature cure cycle is shown in Fig. 3. We have chosen this temperature cycle in order to reproduce the climatic conditions in Algeria, characterized by a cold and humid winter where the temperatures are low and by a hot and dry summer where the temperatures are very high [21]. The mechanical process consists of a longitudinal compression load-unload with different levels of applied load. For a realistic evaluation of the durability of the short concrete column, we follow the technical standards reported by P. Bamforth et al. [22] in which the design strength (design load) labeled Rd is calculated from the ultimate strength value Ru. As such, the value obtained represents the reference value of the short column capacity. In our study, three level of mechanical loading process are retained, each level representing respectively 30%, 50% and 70% of the design strength value Rd calculated. The choice of these three loading levels is intended to reproduce respectively Low-level exploitation, medium-level exploitation and high-level exploitation of concrete structures in service.

## Static compression load-unload testing

All of the measurements were carried out in an Ibertest universal testing machine having a maximum load capacity of 250kN, as shown in Fig.2. Specimens are loaded from 0 kN to the percentage of Rd load defined as indicated in Tab. 3. After that, the measurement is stopped and specimens are unloaded. For each specimen, a controlled loading rate of 3.5 kN/s was used to conduct the compression test.
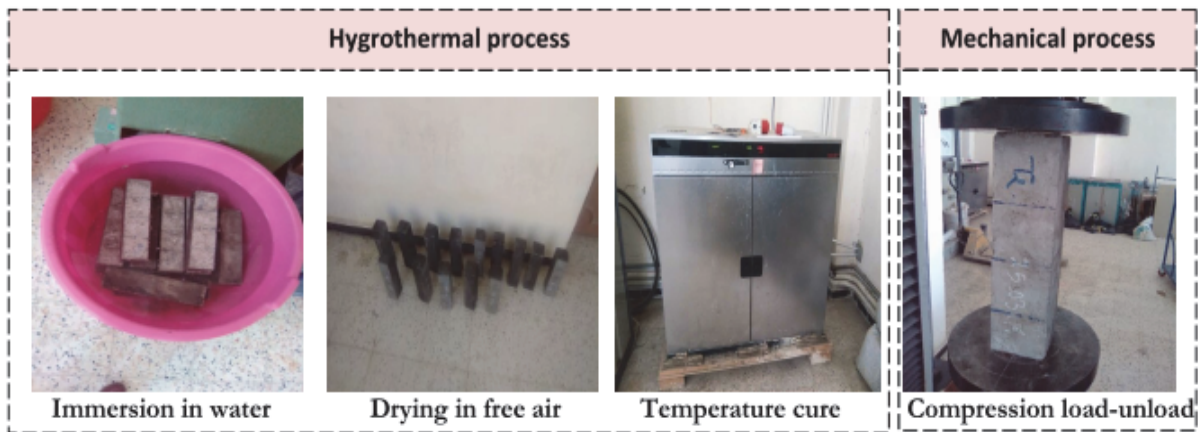
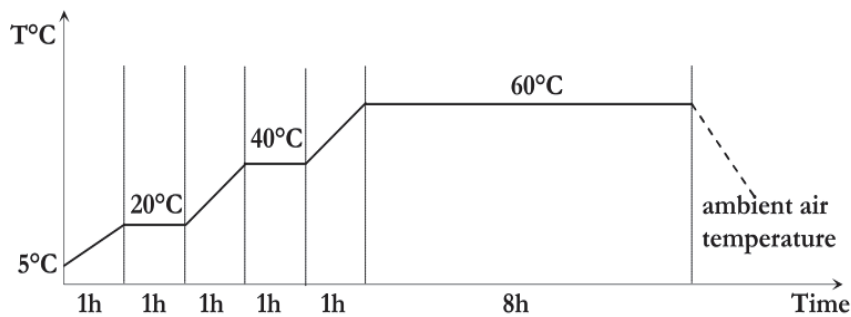Figure 2: Hygrothermo-mechanical aging process.



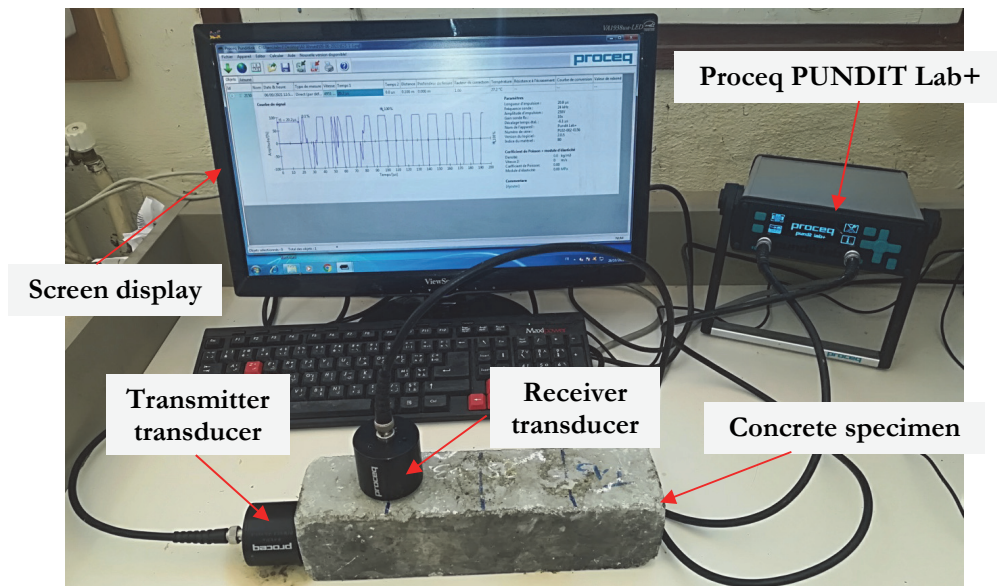Figure 3: Temperature cure process.



Figure 4: Principle and main components of UPV measurements Proceq PUNDIT Lab+.

*Ultrasonic pulse velocity (UPV) testing procedure*

To monitor the behavior of the concrete element in service, over a long period, it was imperative that these tests must be nondestructive. UPV testing of concrete is an effective non-destructive testing method for quality control of concrete, and detecting damages in structural's components [23, 24, 25, 26, 27]. UPV test procedure is given in ASTM C597. The test consists of measuring the time required for a pulse of ultrasonic stress-wave energy to travel through a concrete member.

As shown in Fig. 4, Proceq Portable Ultrasonic Non-destructive Digital Indicating Test (PUNDIT Lab+ ) is used for this purpose. Two transducers, one as transmitter and the other one as receiver, are used to send and receive 54 kHz frequency. The velocity of the wave is measured by placing two transducers, one on each side of concrete element. In order to ensure effective transfer of the wave between concrete and transducer a thin grease layer is applied to the surface of transducer. For each specimen, five measurement points were selected as shown in Fig. 5. Three measurement points along its length were selected for transversal direction. One point is selected in the longitudinal direction while the third is chosen to be used for the semi-direct measurement. To reduce the influence of error and to ensure the repeatability of results, for each measurement point, three measures were made.
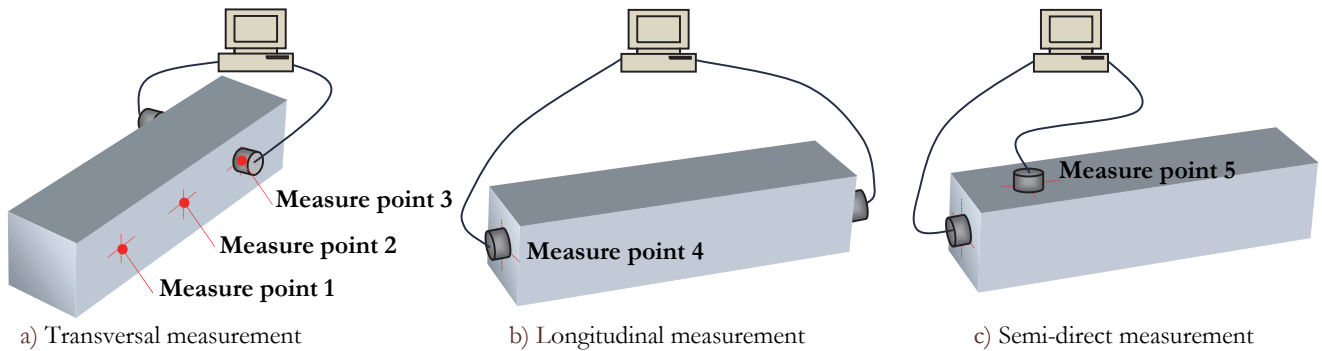


a) Transversal measurement       b) Longitudinal measurement       c) Semi-direct measurement

Figure 5: Different positions of transducer placement used for UPV measurements.

## QUANTIFICATION OF AGEING DEGRADATION OF CONCRETE SHORT COLUMN SPECIMENS

As already indicated in the introduction, to quantify degradation of concrete specimens, we combine UPV testing and compression testing.

*Initial ultrasonic pulse velocity results (before starting aging process)*

Results of the statistical analysis for velocities of ultrasonic waves propagating through the concrete short column, measured before starting the aging process are summarized in the Tab. 4 and shown in Fig.6.It can be seen from Fig. 6 that all measurements present an asymmetrical distribution. In fact, as observed from Tab.4, longitudinal measurements distribution presents a negative value of skewness coefficient. It means that, the longitudinal UPV measurements values spread out more to the left of the sample mean than to the right. In the other hand, transversal and semi-direct measurements distributions present a positive value of skewness coefficient what indicates the UPV measurements values spreads out more to the right of the sample mean. The coefficient of variation Cv is a statistical measure of the relative dispersion of data points in a sample around the mean. It represents the ratio of the standard deviation Std to the mean multiplied by 100.The higher the Cv, the greater the dispersion in the variable. As we can see in Tab. 4, the maximal value of the coefficient of variation is less than 5.6%. This indicates that we do not observe a high dispersion of UPV measurements.

| Configuration measurement | Sample size | Mean | Median | Mode | Max | Min | Skewness | Kurtosis | Std | Cv |
|---|---|---|---|---|---|---|---|---|---|---|
| Longitudinal | 42 | 4680.76 | 4710 | 4719 | 4845 | 4494 | -0.18 | -0.65 | 86.96 | 1.8% |
| Transversal | 126 | 4955.63 | 4898.5 | 4895 | 5312 | 4730 | 1.24 | 0.57 | 124.60 | 2.5% |
| Direct* | 168 | 4886.91 | 4892 | 4895 | 5312 | 4494 | 0.22 | 0.25 | 166.43 | 3.4% |
| Semi-direct | 42 | 5172.14 | 5053 | 5052 | 5942 | 4785 | 1.11 | 0.46 | 289.08 | 5.5% |

Table 4: Statistical parameters of UPV measurements. (*) correspond to the longitudinal and transversal measurements results obtained over the same length of time

a) Longitudinal measurements

b) Transversal measurements

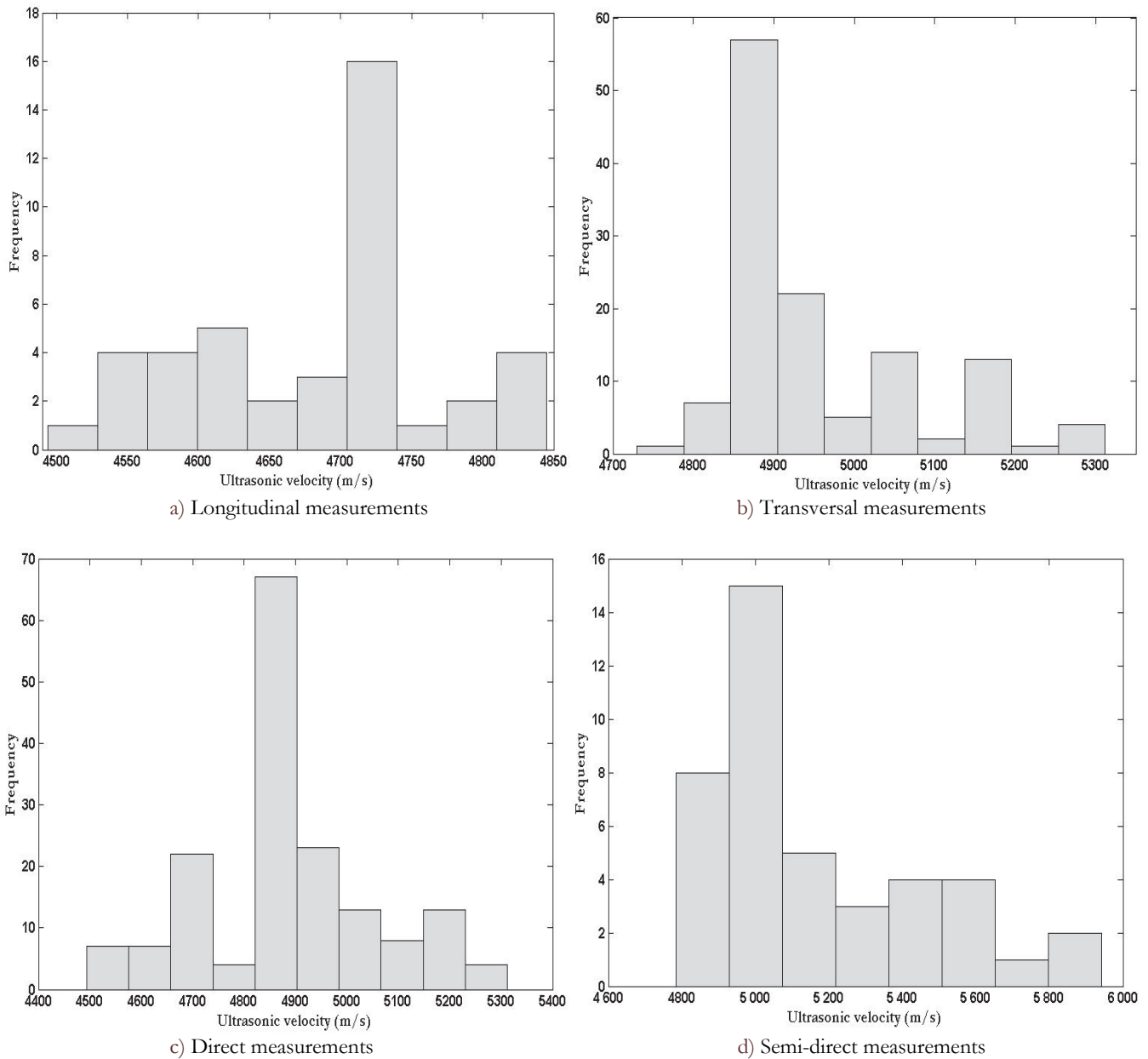c) Direct measurements

d) Semi-direct measurements

Figure 6: Frequency histogram of ultrasonic velocities measured before starting aging process

*Ultrasonic pulse velocity time evolution (after aging process)*

Evolution of the ultrasonic wave velocities, propagating through the concrete short column specimens under the three loading levels 30%, 50% and 70% of design strength Rd, measured during the hygrothermo-mechanical aging process are shown in Fig.7. Results are presented in terms of the ratio of the instantaneous ultrasonic wave velocity UPV of damaged material measured after n cycles of the aging process to the origin ultrasonic wave velocity UPVo of undamaged material measured before starting the aging process. As illustrated in Fig. 7, for all specimens, after n cycles of the aging process there is an attenuation of ultrasonic wave velocity. It represents the response of concrete short column specimens to the degradation of internal properties. As we can see from Fig. 7, from the cycle 1 to the cycle 20, the attenuation of ultrasonic wave velocity is low for specimens loaded with 30% of Rd. from the cycle 1 to the cycle 14, the attenuation of ultrasonic wave velocity is low for specimens loaded with 50% of Rd. from the cycle 1 to the cycle 10, the attenuation of ultrasonic wave velocity is low for specimens loaded with 70% of Rd. After that for all specimens, the attenuation of ultrasonic wave velocity is more notable and increases with the increasing of number of aging cycles. Fig. 7 shows also

that the attenuation of ultrasonic wave velocity obtained after n cycles, for specimen loaded with 70% of Rd is greater than the attenuation of ultrasonic wave velocity obtained after n cycles for specimens loaded with 50% and 30% of Rd.
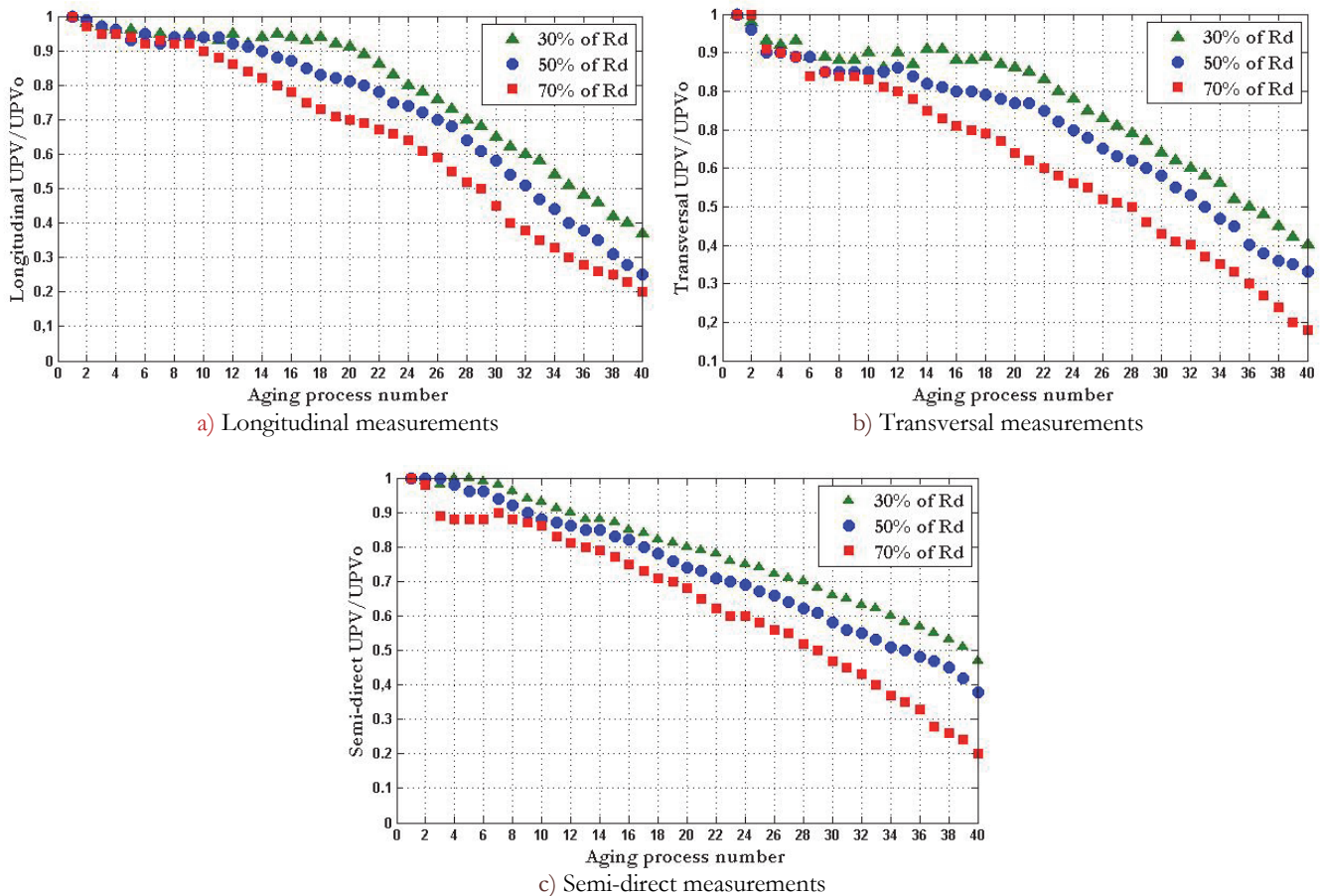


a) Longitudinal measurements

b) Transversal measurements

c) Semi-direct measurements

Figure 7: Time evolution of the UPV according to load level applied

Evolution of the ultrasonic wave velocities, propagating through the concrete short column specimens according to the three exposure conditions; hygrothermal process, mechanical process and the hygrothermo-mechanical process are shown in Fig. 8. Results are presented in terms of the ratio of the instantaneous ultrasonic wave velocity UPV of damaged material measured after n cycles of the aging process to the origin ultrasonic wave velocity UPVo of undamaged material measured before starting the aging process. As illustrated in Fig. 8, for all specimens, after n cycles of the aging process there is an attenuation of ultrasonic wave velocity. As we can see from Fig. 8, the attenuation of ultrasonic wave velocity obtained after n cycles, for specimen under the hygrothermo-mechanical aging process and mechanical aging process are significantly greater than the attenuation of ultrasonic wave velocity obtained after n cycles for specimens under the hygrothermal aging process.

The decay curve of ultrasonic wave velocity of all specimens, as shown in Fig. 8, exhibits generally different stage behavior. In fact, As shown in Fig. 8, from the cycle 1 to the cycle 14, the attenuation of ultrasonic wave velocity is low for the specimens under the mechanical aging process. After the cycle 14, the attenuation of ultrasonic wave velocity becomes notable and increases with the increase of the number of cycles. In case of specimens under the hygrothermal aging process, there is slightly effect on the attenuation of ultrasonic wave velocity.

Evolution of the ultrasonic wave velocities, propagating through the concrete short column specimens with three values of the slenderness ratio h/b under the hygrothermo-mechanical aging process loaded with 70% of Rd, are shown in Fig. 9. As a reminder, h and b represent respectively the height and the width of specimens. Results are presented in terms of the ratio of the instantaneous ultrasonic wave velocity UPV of damaged material measured after n cycles of the aging process to the origin ultrasonic wave velocity UPVo of undamaged material measured before starting the aging process. As illustrated in Fig. 9, for all specimens, after n cycles of the aging process there is an attenuation of ultrasonic wave velocity. As we can see from Fig. 9, from the cycle 1 to the cycle 10, the attenuation of ultrasonic wave velocity is low.

After the cycle 10, particularly for specimens with the slenderness ratio equal 2 and 4, the attenuation of ultrasonic wave velocity is more notable. In case of specimens with slenderness ratio equal 1, the attenuation of ultrasonic wave velocity becomes notable after the cycle 16.

When we compare the attenuation of specimens with slenderness ratio 4, 2 and 1 after aging process, the ratio UPV/UPVo equal respectively 0.2, 0.24 and 0.27. Although this difference is small, it still indicates that the h/b ratio has an effect on the behaviour of specimens.
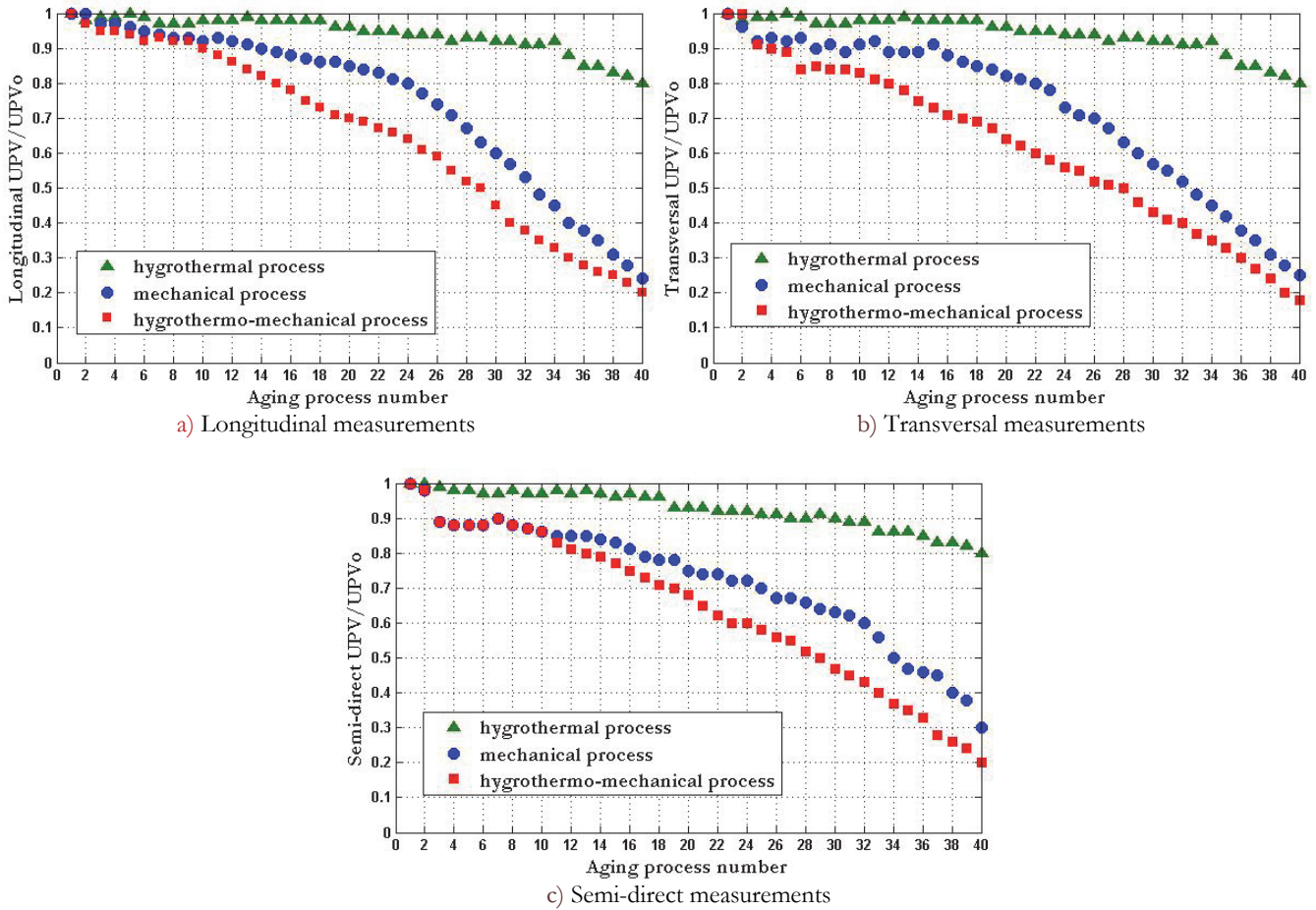


a) Longitudinal measurements

b) Transversal measurements

c) Semi-direct measurements

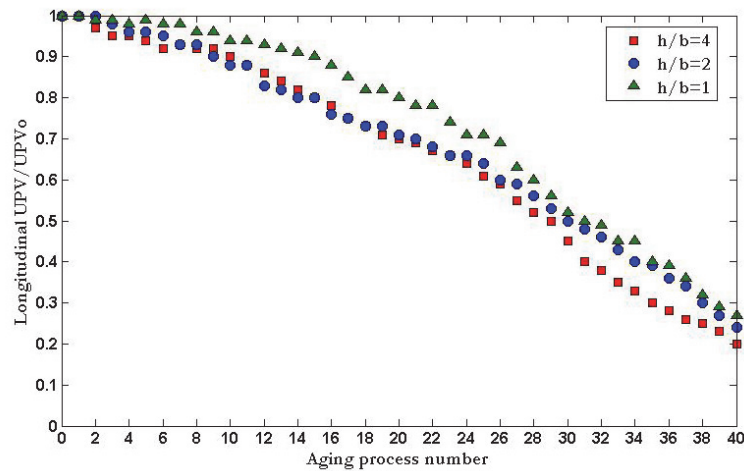Figure 8: Time evolution of the UPV for specimen loaded with 70% of Rd according to the exposure conditions



Figure 9: Time evolution of the longitudinal UPV according to the specimen's slenderness ratio h/b.

*Damage of short concrete column according to UPV measurements*

The damage variable D can be defined with ultrasonic wave velocity as $D=1-(UPV/UPV_o)^2$, where UPV is the instantaneous ultrasonic wave velocity of damaged material after n cycles of aging process and $UPV_o$ is the origin ultrasonic wave velocity of undamaged material before starting the aging process [28].As illustrated in Fig. 10 and Fig. 11, the damage variable D of all concrete short column specimens increases with the increasing number of cycles. As we can see from Fig. 10, the damage D obtained after aging cycles, for specimen loaded with 70% of Rd is greater than the damage D obtained for specimens loaded with 50% and 30% of Rd.



a) Longitudinal measurements
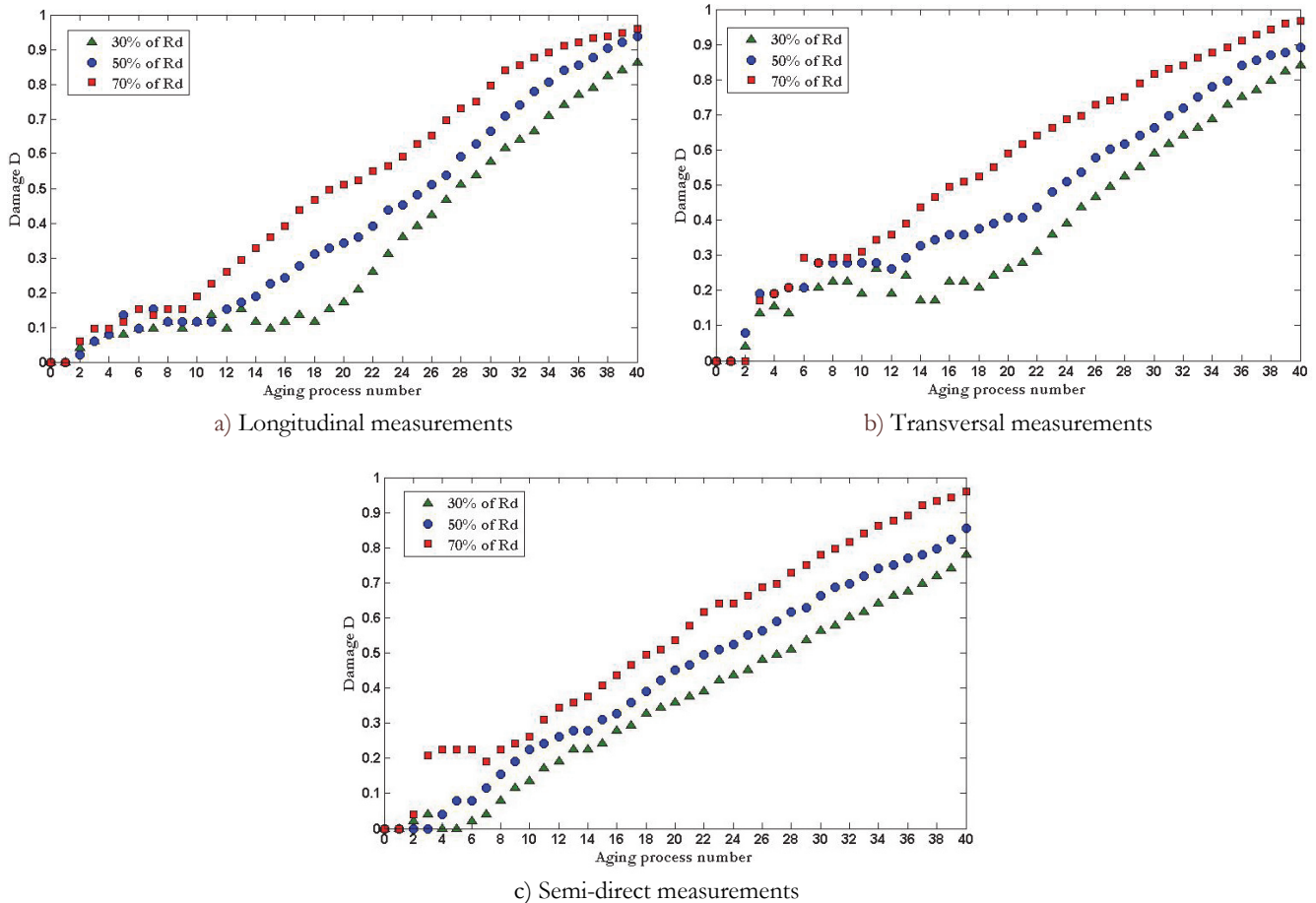
b) Transversal measurements

c) Semi-direct measurements

Figure 10: Damage time evolution according to loading level applied

It must be indicated that for specimens loaded with 50% and 70% of Rd, the final damage value is practically the same in case of longitudinal measurement, whereas it is different in the case of transversal and semi-direct measurements. As we can see from Fig. 11, the damage D obtained after aging cycles, for specimen loaded under the hygrothermo-mechanical process is greater than the damage D obtained for specimens under the mechanical process. It must be indicated that the final value of the damage after 40 cycles is practically the same. In case of specimens under the hygrothermal process, the damage value is less significant compared to the two other specimens.

*Load-displacement curve results*

In this section, we report on our study of the damage behavior of specimens is studied with using the destructive test. Our analysis is based on the load-displacement curve obtained with longitudinal compression test. As an example, we show in Fig. 12 a typical experimental load-displacement curve obtained. At the beginning of the aging process, curves are practically parallel while at the end of aging process there is a larger and larger displacement going from 0.6 to 1.8 mm. Fig. 13 shows the experimental load-displacements curves of the specimens loaded with different value of compression loading, namely 30%, 50%, 70% of Rd and under different exposure conditions namely mechanical and hygrothermo-mechanical aging process. The load-displacements curves obtained have practically the same evolution. It can be observed

that with the increasing of the number of aging cycles, the load-displacement curves are gradually more inclined. This indicates that material stiffness gradually decreases. As a result, for the same value of load there is a larger value of displacement.
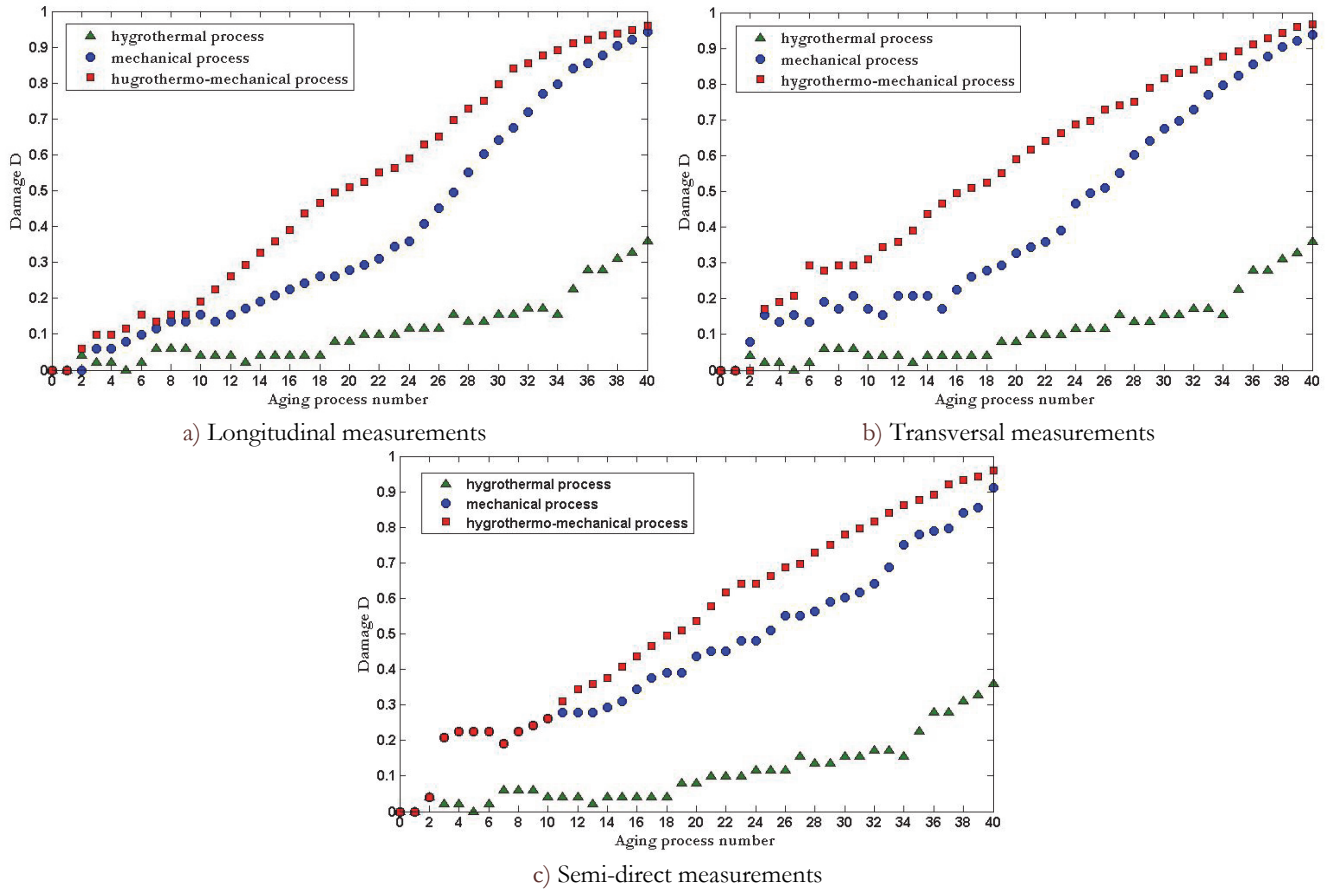
a) Longitudinal measurements

b) Transversal measurements

c) Semi-direct measurements

Figure 11: Damage time evolution according to exposure conditions for specimen loaded with 70% of the design strength Rd;
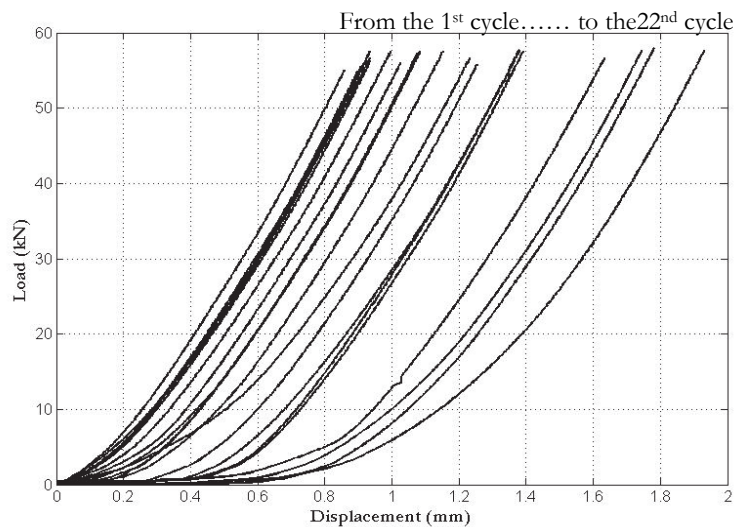
Figure 12: Load-Displacement curve of concrete specimen loaded with 70% of the design strength Rd.

a) Mechanical aging with 30% of Rd

b) Mechanical aging with 50% of Rd

c) Hygrothermo-mechanical aging with 50% of Rd
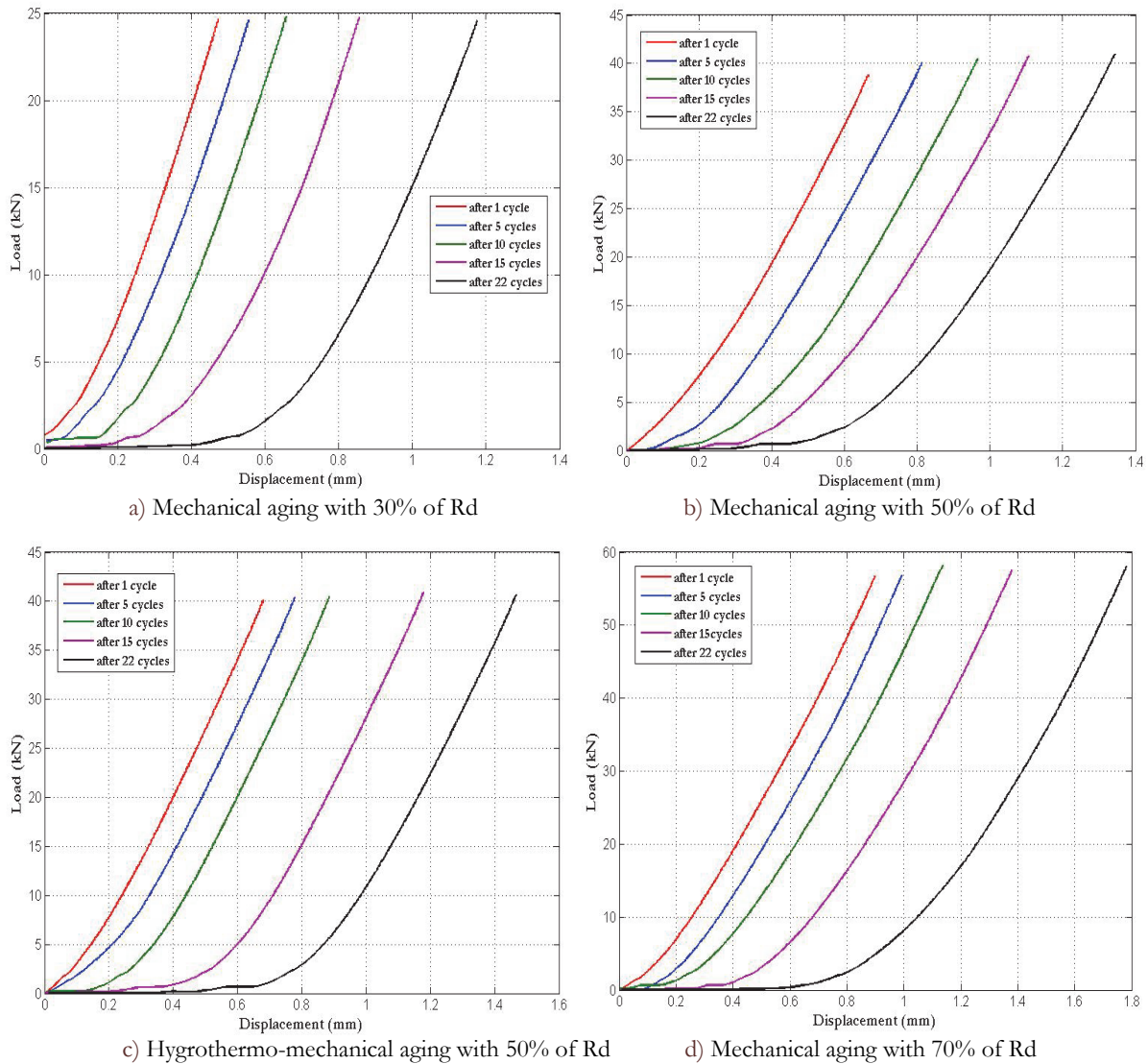
d) Mechanical aging with 70% of Rd

Figure 13: Load-displacement curves obtained for different specimen.

We present in Fig.14 the time evolution of the load-displacement curve of the concrete short column specimens for different level of load applied. First, it can be seen that for the first cycle, load-displacement curves are the same. This indicates that there is no notable damage early in the aging process. This confirms that there is not a high variability of our concrete quality. This agrees well with the statistical analysis of the initial ultrasonic pulse velocity measurements presented above. Second, as the number of aging process increases, the difference between the curves is more notable. This indicates that after several aging process cycles, the degradation was more notable.

Fig. 15 shows the time evolution of the load-displacement curve of the concrete short column specimens for different exposure conditions. As observed using Fig. 15, we see that at the start the aging process, load-displacement curves remain the same. In addition, just as observed above, as the number of aging process increases, the difference between the curves grows.

To illustrate the behavior of the short concrete column specimens under different loading and exposures conditions, load-displacement curves obtained after the 22nd aging process, are compared in Fig. 16 to the load-displacement curve of the reference specimen obtained from characterization of the concrete short column specimens. It can be observed that the load-displacement curves obtained after aging process are under the reference specimen curve. This difference can be explained by the loss of the rigidity of specimens due to the degradation that has occurred gradually with the aging process. It can be seen also from the Fig. 16 that this difference increases when level of loading increases, and when we consider a coupled hygrothermal and mechanical aging process.
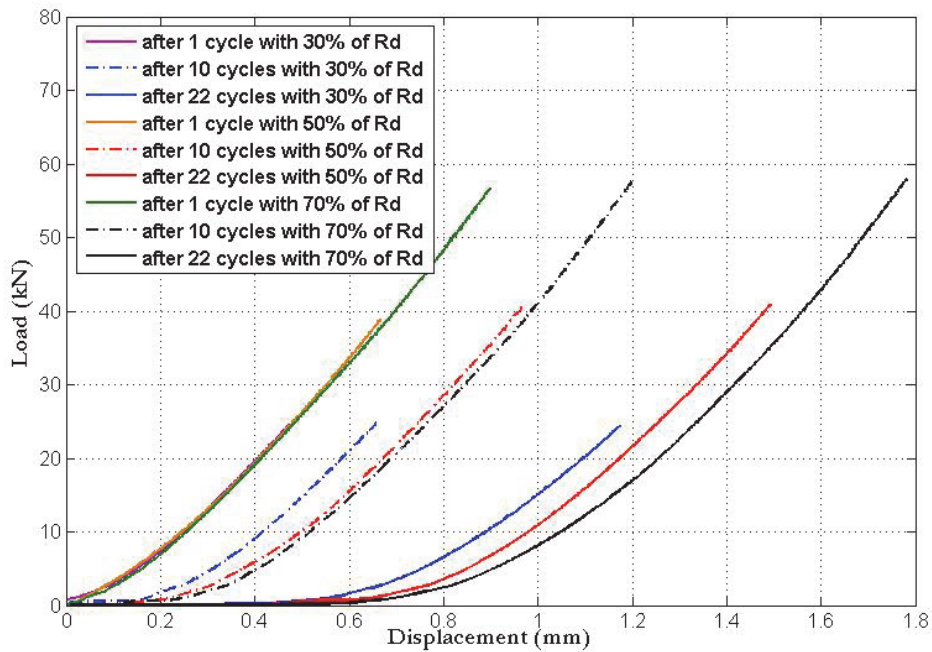
Figure 14: Load-displacement curve time evolution of specimens according to level of load.
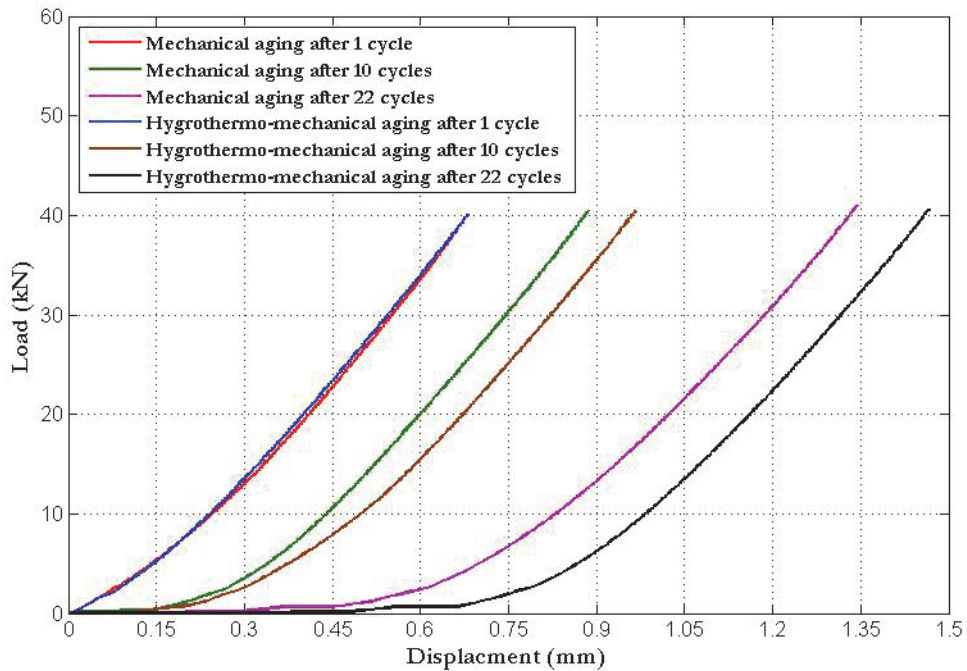


Figure 15: Load-displacement curve evolution of specimens according to type of exposure conditions.

*Damage of short concrete column according to the compression test results*

Damage variable D can be expressed as the loss of stiffness. In this case, the damage variable is defined with Young's modulus as $D=1-E_f/E_0$, where $E_f$ is the Young's modulus of damaged material after n cycles of aging process and $E_0$ is the Young's modulus of undamaged material before starting the aging process [28]. By considering the shape of the curves in Fig 12 we define two Young's moduli, namely the initial and final Young's modulus. The initial Young's modulus is calculated in the first part of the load displacement curve after 5kN and the final Young's modulus is calculated in the second part of the load displacement curve. Fig. 17 shows the time evolution of damage variable D for concrete short column specimens under hygrothermo-mechanical aging process loaded with 70% of Rd. As we can see from Fig. 17, the

damage variable D of specimens increases with the increasing number of cycles. Fig. 7 shows that from cycle 1 to cycle 9, the value of the damage is low and equal 0.1. The damage calculated by considering the initial and final Young's modulus is practically the same. From the cycle 10 the difference becomes notable. After 22 aging cycles, the damage obtained by considering the initial Young's modulus equal 0.67 and the damage obtained by considering the final Young's modulus equal 0.5. We present in Fig. 18 the time evolution of cracks in specimen loaded with 70% of the design load Rd. At the beginning of the aging process as shown in Fig. 18-a no more cracks are observed. As shown in Fig 18-b and 18-c, as aging cycles increased, more cracks are observed. At the end of aging process as shown in Fig. 18-d cracks propagate and appear in all regions of the short column specimens.
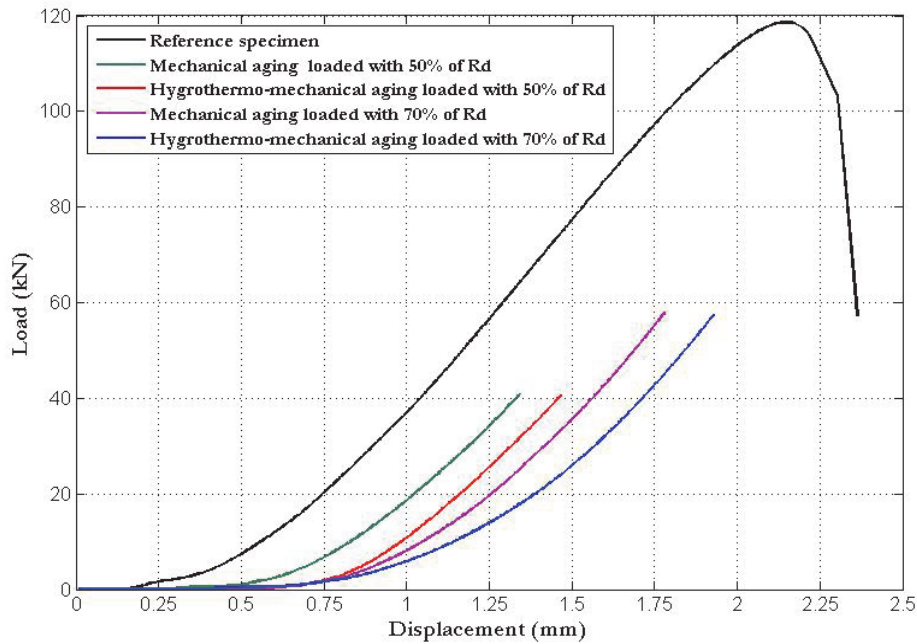
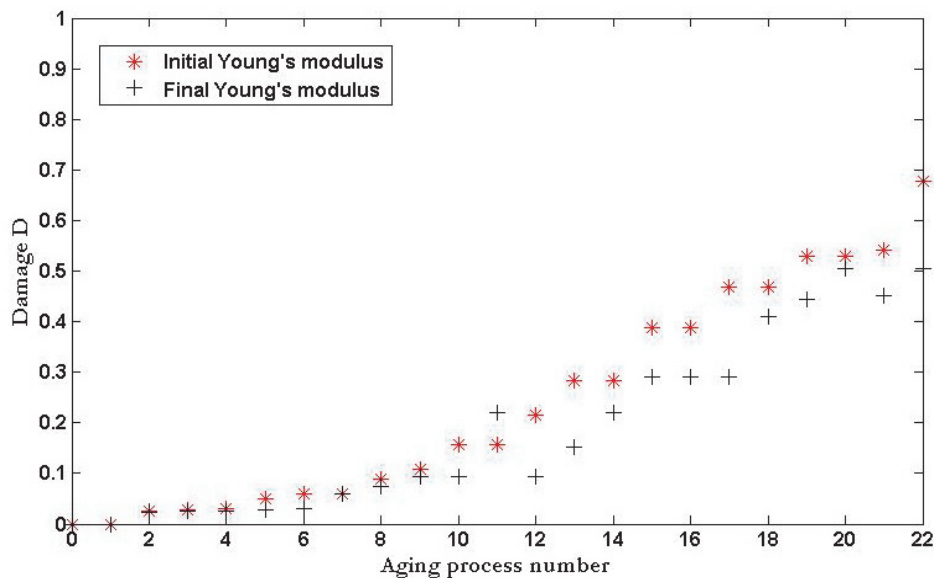Figure 16: Load-Displacement curve evolution of specimens compared to reference concrete.

Figure 17: Time evolution of damage variable for specimen under hygrothermo-mechanical aging process loaded with 70% of Rd.

In Fig. 19, we show the time evolution of the damaged specimen for different loading levels. The damage is defined by the ratio d/dmax where d represents the displacement measured in compression loading process and dmax represents the

maximal displacement obtained in the compression test. The ratio, d/dmax, increases after aging process. This indicates that there is a lost of rigidity. Fig. 20 represents a graph showing the specimen loaded with 50% of Rd, damage time evolution according to exposure conditions. The damage is also defined by the ratio d/dmax. Fig. 20 shows that the ratio d/dmax is practically the same when we start the aging process. Progressively, after several cycles of the aging process, the ratio d/dmax corresponding to the coupled hygrothermo-mechanical aging process is slightly higher that the ratio d/dmax corresponding to the mechanical aging process.

*Comparison between the UPV testing and compression testing measurements*
Fig. 21, shows the time evolution of the damage variable according to the different formulations of the damage D. As we can see, the damage calculated according to the transversal and semi-direct UPV measurement is greater than the damage calculated according to longitudinal UPV measurements and compression test particularly from the cycle 3 to the cycle 17. After that the difference between the different formulations of D becomes low. In fact, the maximum difference equal 0.26 is obtained in the cycle 6 and cycle 12 when the minimum difference equal 0.08 is obtained in the cycle 20. Globally, with the increasing of the aging cycles, UPV testing measurements agree well with the compression testing results.
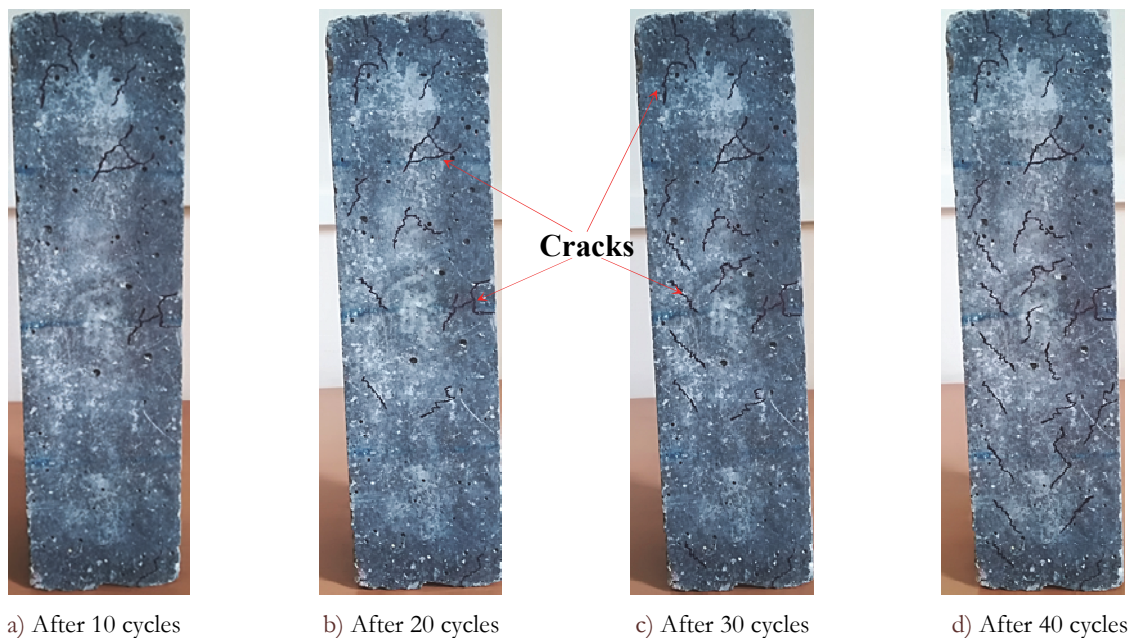


| a) After 10 cycles | b) After 20 cycles | c) After 30 cycles | d) After 40 cycles |

Figure 18: Time evolution of cracks for specimen loaded with 70 % of design strength Rd.
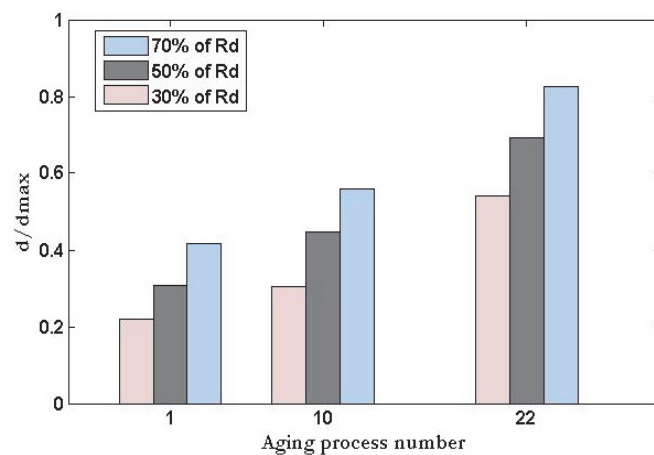


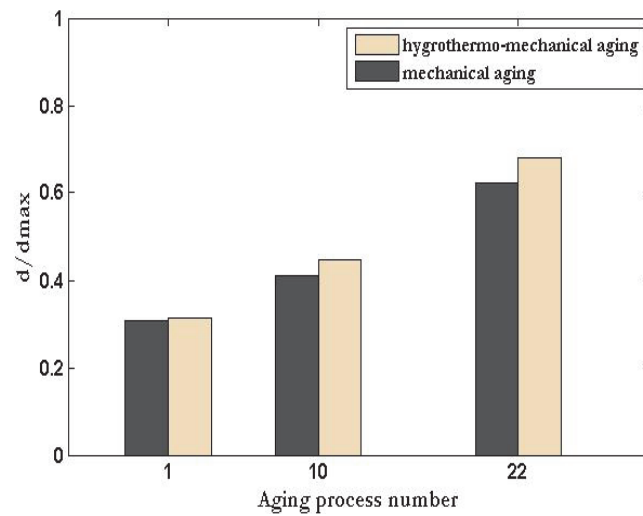Figure 19: Damage time evolution according to loading level.

Figure 20: Damage time evolution according to exposure conditions for specimen loaded with 50% of the design strength Rd.
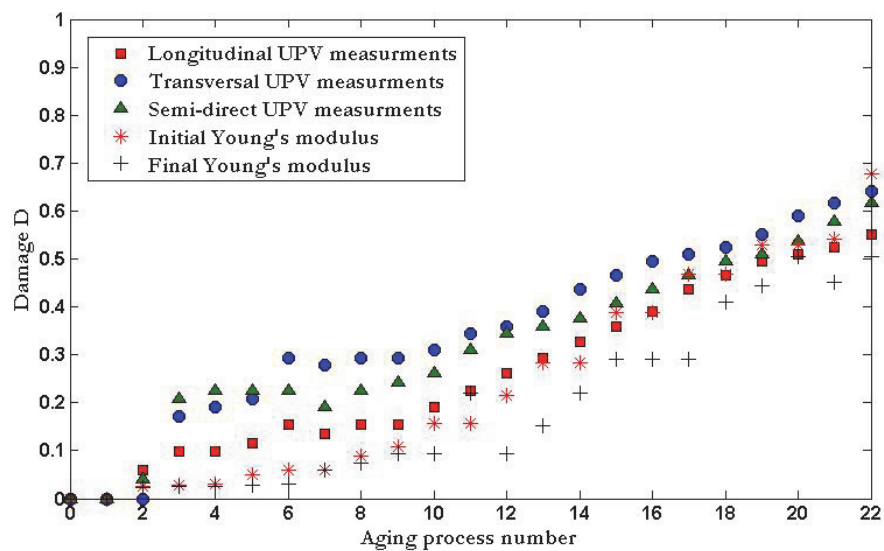


Figure 21: Comparison between damage variable evaluation methods for specimen loaded with 70% of the design strength Rd.

## CONCLUSIONS

The aim of this work is to study the combined effects as expected in real-life conditions, of the hygrothermal and mechanical exposure conditions on civil engineering structures. This experimental work illustrates a combined non-destructive (NDT) assessment and destructive (DT) assessment of concrete prismatic short column deterioration under a combined effect of the two alternating processes: mechanical loading (compression load-unload) and hygrothermal exposures conditions (immersion in water for 24 hours, evaporation of excess water in ambient air temperature for 24 hours and finally temperature cure cycle). For detecting damages in concrete specimens, ultrasonic pulse velocity (UPV) testing and compression testing are used. Based on the experimental observations of the behavior of short concrete columns under these two alternating processes, it can be observed that:

- For all specimens, after n cycles of the aging process there is an attenuation of ultrasonic wave velocity. this observation agrees well with results obtained from [29].
- At the beginning of the aging process the ultrasonic pulse velocities decrease slightly while at the end, the decrease is notable. In fact, the decay curve of ultrasonic wave velocity of all specimens, exhibits generally three-

stage behavior particularly in case of specimens under mechanical and hygrothermo-mechanical aging process. it is not easy to distinguish between these three stages, but this corresponds to the results found by [28].

- The hygrothermal aging process has a slight effect on the ultrasonic wave propagation velocity compared to the effect of the loading process and/or the effect of the combined hygrothermo-mechanical process.
- The attenuation of ultrasonic wave velocity increases when load level applied increases.
- The slenderness ratio effect on the attenuation of ultrasonic velocities measured in this work appears slightly according to the values of h/b considered. For more comprehension, it will be interesting to investigate the high values of this ratio.
- At the beginning of the aging process, load-displacement curves remain the same. As the number of aging process increases, the difference between the curves becomes more notable.
- Globally, with the increasing of the aging cycles, UPV testing measurements agree well with the compression testing results.
- The decay curve of ultrasonic wave velocity is capable of reflecting the evolution process of degradation

## ACKNOWLEDGEMENTS

## REFERENCES

[1] Sanjeev K.V., Sudhir S.B., Saleem A. (2013). Estimating residual service life of deteriorated reinforced concrete structures., American J. of Civ. Eng. and Architecture, 1(5), pp. 92-96. DOI:10.12691/ajcea-1-5-1

[2] Gjørv, O.E. (2011). Durability of concrete structures., Arab J Sci. Eng., 36, pp. 151–172.
DOI: 10.1007/s13369-010-0033-5.

[3] Stochino et alii, F. (2018). Assessment of RC Bridges integrity by means of low-cost investigations, Frattura ed Integrità Strutturale, 46, pp. 216-225. DOI: 10.3221/IGF-ESIS.46.20.

[4] Pijaudier-Cabot, G., Khalil, H., Loukili, A., Omar, M. (2004). Ageing and durability of concrete structures., Degradations and Instabilities in Geomaterials, 461 Springer, pp. 255-286.
DOI: 10.1007/978-3-7091-2768-1_9.hal– 01572477.

[5] Somasundaram, V., Calvin, K.C. (2008). Aging degradation of mechanical structures., J. of mechanics of materials and structures, 3(10). pp. 1923-1938.

[6] Pinto, S., Hobs, S., Hover, K. (2002). Accelerated aging of concrete: a literature review., Federal Highway Administration, https://trid.trb.org/view/706737. 94 p.

[7] Wan-Wendner, R. (2018). Aging concrete structures: a review of mechanics and concepts, Journal of Land Management, Food and Environment, 69 (3), pp. 175–199. DOI: 10.2478/boku-2018-0015.

[8] Qifang, X., Lipeng, Z., Shenghua, Y., Baozhuang, Z., and Yaopeng, W. (2019). Effects of high temperatures on the physical and mechanical properties of carbonated ordinary concrete., Adv. In Mater. Sci. and Eng.
DOI: 10.1155/2019/5753232

[9] Bochen, J., Slusarek, J. (2020). Analysis of resistance to accelerated aging of the top layer of small-sized concrete elements. A case study., Const. and Build. Mater. 264, 120211, DOI: 10.1016/j.conbuildmat.2020.120211.

[10] Künzel H., Holm, A. Krus, M. (2008). Hygrothermal properties and behaviour of concrete., WTAAlmanach, pp. 161.

[11] Kallel, H., Carré H., Laborderie, C., Masson, B., Tran, N. (2016). Effects of the hygrothermal conditions on the fracture energy of the concrete., Key Eng. Materials., 711, pp. 397-403.
DOI: 10.4028 /www .scientific.net /KEM.711.397.

[12] Mateos, A. et al. (2020). Structural response of concrete pavement slabs under hygrothermal actions., Const. and Build. Mater., 243, 118261. DOI: 10.1016/j.conbuildmat.2020.118261.

[13] Mukhtar, F.M., Peiris, A. (2021). FRP-concrete bond performance under accelerated hygrothermal conditions., Const. and Build. Mater., 270, DOI: 10.1016/j.conbuildmat.2020.121403.

[14] Zdenek, P., Milan, J., (2018). Creep and hygrothermal effects in concrete structures,

DOI: 10.1007/978-94-024-1138-6.

[15] D.P. Chen 1 and all. (2015) Advances in multi-scale simulation of hygro-thermo-mechanical deformation behavior of structural concrete., Int J. of Civil Eng., 13. pp. 267-277.
DOI: 10.22068/IJCE.13.3.267[URL:http://ijce.iust.ac.ir/article -1-676-en.html].

[16] Karavokyros, L., George Batis, G., Katsiotis, N., Tzanis, N, Beazi-Katsioti, M. (2020). Durability of reinforced concrete beams under simultaneous flexural load in corrosive environment. J. of Mat. Sci. and Chemical Eng, 8 (4). pp. 32-45. DOI: 10.4236/msce.2020.84003.

[17] Gawina, D., Pesavento, F. Schreflerb, A. (2003). Modelling of Hygro-Thermal Behaviour of Concrete at High Temperature with Thermo-Chemical and Mechanical Material Degradation. Comput. Methods Appl. Mech. Engrg. 192(13-14), pp. 1731-1771. DOI:10.1016/S0045-7825(03)00200-7.

[18] Kim, J.-K., Hun Han, S. and Kyun Park, S. (2002). Effect of temperature and aging on the mechanical properties of concrete. Cement and Concrete Research, 32(7), pp. 1095–1100. DOI:10.1016/s0008-8846(02)00745-7.

[19] Baroghel-Bouny, V., Thiery, M., Dierkens, M.and Wang, X. (2016) Aging and durability of concrete in lab and in field conditions – pore structure and moisture content gradients between inner and surface zones in RC structural elements, Journal of Sustainable Cement-Based Materials, 6(3), pp. 149-194, DOI: 10.1080 /21650373.2016.1169232.

[20] Ola Adel, Q., (2018). A review paper on specimens size and shape effects on the concrete properties, Int. J. of Recent Adv. in Sci. and Tech.; 5 (3), pp. 13-25. DOI: 10.30750/ijarst.533.

[21] Salah Sahabi, A., Matzarakis, A., (2017). Seasonal Regional Differentiation of Human Thermal Comfort Conditions in Algeria, Advances in Meteorology, DOI: 10.1155/2017/9193871.

[22] Bamforth, P., Chisholm, D., Gibbs, J., Harrison, T. (2008). Properties of Concrete for use in Eurocode 2. 59p.

[23] Helal, J., Sofi, M., Mendis, P. (2015). Non-destructive testing of concrete: a review of methods., Elect J. of Stru. Eng., 14 (1), pp. 97-105.

[24] Karaiskos, G., Deraemaeker, A., Aggelis, D.G., Van Hemelrijck, D. (2015). Monitoring of concrete structures using the ultrasonic pulse velocity method., Smart Mater. Struct., 24, 113001. DOI: 10.1088/0964-1726/24/11/113001.

[25] Ndagi, A., Umar, A., Hejazi, F., Jaafar, M.S. (2019). Non-destructive assessment of concrete deterioration by ultrasonic pulse velocity: A review., IOP Conference Series: Earth and Envir. Sci., 357, 012015.
DOI: 10.1088 /1755-1315/357/1/012015.

[26] Nandipati, S., Ravi Kumar, M., Barkavi, T., Natarajan, C. (2018). Structural health monitoring: detection of concrete flaws using ultrasonic pulse velocity., J. of Buil. Pathology and Rehabilitation, 3.
DOI: 10.1007/s41024-018-0036-2.

[27] Presa, L., Costafreda, J.L., Martín, D.A. (2021). Correlation between uniaxial compression test and ultrasonic pulse rate in cement with different pozzolanic additions., Appl. Sci., 11, 3747. DOI: 10.3390/app11093747.

[28] Xiao, J.-Q., D.-X. Ding, F.-L. Jiang, and G. Xu. (2010). Fatigue damage variable and evolution of rock subjected to cyclic loading. Int. J. Rock Mech. Min. Sci. 47 (3), pp. 461 – 468. DOI: 10.1016/j.ijrmms.2009.11.003.

[29] A.M. Mahmoud et al (2010). Non-destructive ultrasonic evaluation of CFRP–concrete specimens subjected to accelerated aging conditions, NDT&E International 43, pp. 635–641. DOI: 10.1016/j.ndteint.2010.06.008.